Author's Accepted Manuscript

www.elsevier.com/locate/csr

Predicting the large-scale consequences of offshore wind turbine array development on a north sea ecosystem

Johan van der Molen, Helen C.M. Smith, Paul Lepper, Sian Limpenny, Jon Rees

PII: S0278-4343(14)00200-3
DOI: http://dx.doi.org/10.1016/j.csr.2014.05.018
Reference: CSR3055

To appear in: *Continental Shelf Research*

Received date: 23 December 2013
Revised date: 19 May 2014
Accepted date: 28 May 2014

Cite this article as: Johan van der Molen, Helen C.M. Smith, Paul Lepper, Sian Limpenny, Jon Rees, Predicting the large-scale consequences of offshore wind turbine array development on a north sea ecosystem, *Continental Shelf Research,* http://dx.doi.org/10.1016/j.csr.2014.05.018

Predicting the large-scale consequences of offshore wind turbine array development on a North Sea ecosystem

Johan van der Molen[1], Helen C.M. Smith[2], Paul Lepper[3], Sian Limpenny[1], Jon Rees[1]

[1] Cefas, Pakefield Road, Lowestoft NR33 0HJ, United Kingdom, johan.vandermolen@cefas.co.uk

[2] College of Engineering, Mathematics and Physical Sciences, University of Exeter, Cornwall Campus, Penryn, Cornwall TR10 9EZ, United Kingdom, h.c.m.smith@exeter.ac.uk

[3] School of Electronic, Electrical and Systems Engineering, Loughborough University, Loughborough LE113TU, United Kingdom, p.a.lepper@lboro.ac.uk

Revised version, May 2014

Abstract

Three models were applied to obtain a first assessment of some of the potential impacts of large-scale operational wind turbine arrays on the marine ecosystem in a well-mixed area in a shelf sea: a

biogeochemical model, a wave propagation model and an acoustic energy flux model. The results of the models are discussed separately and together to elucidate the combined effects. Overall, all three models suggested relatively weak environmental changes for the mechanisms included in this study, however these are only a subset of all the potential impacts, and a number of assumptions had to be made. Further work is required to address these assumptions and additional mechanisms. All three models suggested most of the changes within the wind turbine array, and small changes up to several tens of km outside the array. Within the array, the acoustic model indicated the most concentrated, spatially repetitive changes to the environment, followed by the SWAN wave model, and the biogeochemical model being the most diffuse. Because of the different spatial scales of the response of the three models, the combined results suggested a spectrum of combinations of environmental changes within the wind turbine array that marine organisms might respond to. The SWAN wave model and the acoustic model suggested a reduction in changes with increasing distance between turbines. The SWAN wave model suggested that the biogeochemical model, because of the inability of its simple wave model to simulate wave propagation, over-estimated the biogeochemical changes by a factor of 2 or more. The biogeochemical model suggested that the benthic system was more sensitive to the environmental changes than the pelagic system.

Keywords: wind farm, marine ecosystem, model, wave, noise

1 Introduction

Over the last decade, there has been rapid expansion of the offshore wind sector since the UK's first offshore turbines were constructed off Blyth Harbour, off the Northumberland Coast (Grainger and Thorogood, 2001). This set the scene for offshore wind to play a major role in ensuring the UK's energy security and in meeting the Government's target of achieving 15% of energy consumption from

renewable sources by 2020 (EU, 2009). Since 2000, there have been five rounds of leasing use of areas of sea bed associated with the development of offshore wind turbine arrays around the UK; the size of which have increased in scale and technical complexity as the industry has developed.

DECC (the Department for Energy and Climate Change) completed its latest Offshore Energy Strategic Environmental Assessment in 2011 (OESEA2, 2011). This assessment concluded that up to 33 GW of offshore wind development could take place within the UK Renewable Energy Zone and English and Welsh Territorial Waters up to a depth of 60m, as long as some areas were avoided (e.g. shipping lanes) and that projects should include any necessary mitigation measures to reduce likely significant adverse impacts on the environment and other users of the sea. The Crown Estate, which grants leases for the use of the UK seabed for offshore renewable energy construction, designed the so-called Round 3 zones. These are large areas of seabed around the UK which The Crown Estate has determined are the places most suitable for offshore wind development. These areas have the potential for large numbers of turbines to be installed; indeed it is likely that some licence applications will include proposals for the installation of several thousand turbines at a rating of up to 8 MW each in a single Zone.

Round 3 Developers are currently undertaking survey work and studies to help them understand the most appropriate locations for offshore wind turbine array projects within the zone. They take into consideration engineering, economics and environmental factors when deciding on the locations of wind turbine arrays. When they have made the decision on the best location for a project, they undertake an Environmental Impact Assessment (and in certain circumstances an Appropriate Assessment), and detailed consultation on the proposal for the wind turbine array.

Due to the recent nature of this industry very little is known about the potential medium to long-term environmental consequences (measured as either positive benefits or negative effects) of placing structures such as wind turbines in high densities in offshore environments around the UK coast. Concerns over the potential impacts include loss of biodiversity due to habitat loss, modifications to existing marine communities through habitat creation, noise, collision risk, changes in sediment transport patterns, shifts in hydrodynamic regimes and electromagnetic fields (Neil et al., 2009; OSPAR, 2008).

Concerns have also been raised over the potential for large scale effects given the proposed expansion of the offshore wind industry associated with proposed Round 3 developments. Similarly, there has been relatively little work emphasising the potential environmental benefits which may include localised increases in biodiversity and function through new habitat creation leading to increased ecological capacity of the environment, the provision of refuges and the aggregation of commercially important species such as gadoids and crustaceans. There are also likely to be ecosystem benefits as a consequence of renewable energy development through the establishment of potentially large areas of seabed that could be subject to much reduced pressures from shipping, commercial trawling and dredging (Linnane et al., 2000; Gill, 2005; Peterson and Malm, 2006; Wilhelmsson et al., 2006; Fayram and de Risi, 2007; Inger et al., 2009; Langhamer and Wilhelmsson, 2009; Wilson and Elliott, 2009).

In most prospective offshore wind development areas, it is likely that project capacity will be initially limited by hard engineering constraints e.g. cable routes, oil and gas rigs, shipping lanes rather than environmental constraints or by the theoretically available wind resource. However, it is essential, if the growth of the offshore wind sector is not to be inappropriately hindered, that the ecological consequences from project developments can be reliably predicted in advance of development. As with other energy sectors, appropriate array design can, in principle, minimise ecological impact. However, neither impact assessment nor ecosystem modelling impacts of development are trivial activities. Models of impact are only now being developed and involve robust assessment of the physical perturbation of the marine environment and the ecological consequences of such perturbation. Inevitably, some aspects of the physical perturbation are directly associated with the wind energy extraction itself and uninfluenced by the design of the technology but other aspects will be specific to the technology. For example, the form of wind turbine foundations may have an effect upon the nature of the wake behind a wind turbine, but is not associated directly with the energy extraction process. Similarly, the type of foundation is likely to influence underwater sound levels.

This study was initiated to assess the possible large scale ecosystem consequences of a theoretical offshore wind turbine array development at a site in the North Sea using a coupled hydrodynamics-

biogeochemistry model, an acoustic model and a wave model. An ongoing challenge is to establish the extent to which such modelling approaches can be employed to assist with the management of human activities such as proposed offshore renewable energy developments. In this paper, we explore this by first describing the results from a theoretical case study in the North Sea and then examining the potential utility of the modelling methods in meeting future regulatory needs, particularly in relation to managing the large scale expansion of offshore renewable energy developments.

2 Model description

2.1 Biogeochemical model

The coupled physical-biogeochemical model GETM-ERSEM-BFM was used for an initial exploration of the potential effects of the wind energy extraction. GETM (General Estuarine Transport Model) is a public domain, three-dimensional Finite Difference hydrodynamical model (Burchard and Bolding, 2002; www.getm.eu). It solves the 3D partial differential equations for conservation of mass, momentum, salt and heat. The ERSEM-BFM (European Regional Seas Ecosystem Model - Biogeochemical Flux Model) version used here is a development of the model ERSEM III (see Baretta et al., 1995; Ruardij and van Raaphorst, 1995; Ruardij et al., 1997; Vichi et al., 2003; Vichi et al., 2004; Ruardij et al., 2005; Vichi et al., 2007; van der Molen et al., 2013; www.nioz.nl/northsea_model), and describes the dynamics of the biogeochemical fluxes within the pelagic and benthic environment. The ERSEM-BFM model simulates the cycles of carbon, nitrogen, phosphorus, silicate and oxygen and allows for variable internal nutrient ratios inside organisms, based on external availability and physiological status. The model applies a functional group approach and contains four phytoplankton groups, four zooplankton groups and five benthic groups, the latter comprising four macrofauna and one meiofauna groups. Pelagic and benthic aerobic and anaerobic bacteria are also included. The pelagic module includes additional processes over

the oceanic version presented by Vichi et al. (2007) to make it suitable for temperate shelf seas: (i) a parameterisation for diatoms allowing growth in spring, (ii) enhanced transparent exopolymer particles (TEP) excretion by diatoms under nutrient stress, (iii) the associated formation of macro-aggregates consisting of TEP and diatoms, leading to enhanced sinking rates and a sufficient food supply to the benthic system especially in the deeper offshore areas (Engel, 2000), (iv) a Phaeocystis functional group for improved simulation of primary production in coastal areas (Peperzak et al., 1998), and (v) a suspended particulate matter (SPM) resuspension module that responds to surface waves for improved simulation of the under-water light climate. The wave function used to calculate waves in ERSEM-BFM is an equilibrium JONSWAP formulation with shoaling term. This formulation does not account for wave propagation or interactions with structures. SPM concentrations are calculated as proportional to the local wave-induced bed-shear stress, varying linearly with depth, and with an exponential relaxation mechanism that represents delayed settling (Appendix 1). There is no SPM resuspension by currents, and no advection of SPM. The ERSEM-BFM model used here includes a 3-layer benthic module comprising 53 state variables, which enables it to resolve substantially more benthic processes and more detailed benthic-pelagic coupling than other biogeochemical models recently applied to the North Sea (Radach and Moll, 2006; Lenhart et al., 2010).

Physical forcing is a major influence in determining the results of ecological models (e.g., Skogen and Moll, 2005). Such forcing includes components that have local dominance (e.g., air temperature, irradiation, wind speed, sediment resuspension and effects on light climate, and anthropogenic disturbance), and components that include regional and gradient effects (advection of properties). Here, we focus on the effects of local changes in wind speed due to the presence of a large, hypothetical wind turbine array.

2.2 SWAN

SWAN (Simulating WAves Nearshore) is a third-generation phase-averaged spectral wave model, specifically designed for near-shore depth-limited regions (Booij et al., 1999). The software propagates offshore wave conditions, input at the model boundaries as either integrated parameters or spectra, across a user-defined grid of bathymetry to the region of interest. The evolution of the wave energy density spectrum in space and time is calculated by solving the action balance equation, which comprises source terms for energy input into the model (from wind), dissipation (from whitecapping, and shallow-water effects) and redistribution (via triad and quadruplet interactions). As SWAN is specifically designed for use in near-shore regions, shallow water and depth-limited processes including refraction, bottom friction and depth-induced breaking are accounted for, and diffraction in SWAN is represented by a phase-decoupled approach (Holthuijsen et al., 2003). Other optional inputs include variable surface currents, enabling the effects of currents on waves to be accounted for, and varying water levels for regions with a significant tidal range. Physical barriers, with user-defined energy transmission and reflection coefficients, can also be included to represent physical structures such as breakwaters. Further details on the physical processes modelled by SWAN can be found in Booij et al. (1999) and the SWAN User Manual (SWAN Team, 2006).

Although primarily a tool for transforming wave parameters from one location to another, over the last decade SWAN has increasingly been used as an impact assessment tool for marine energy developments. Spectral models such as SWAN provide the ability to predict far-field effects over wide geographic areas, which is beyond the scope of the more hydrodynamically accurate but computationally intensive phase-resolving models used to assess the interaction of waves and individual devices or structures. Studies to date have primarily focused on wave energy developments, e.g. Millar et al. (2007), Smith et al. (2012), Rusu and Guedes Soares (2013). However, a similar approach can be taken with large arrays of offshore wind turbines. Although not designed to extract energy from waves, turbine piles are large structures in the water column that will affect the propagation of waves via blocking, diffraction and reflection. An assessment of impacts on the wave climate is therefore a necessary component of an environmental impact assessment for an offshore wind turbine array. The offshore wind industry is more advanced than

the wave industry, and a significant number of projects around the world have been installed, with many more currently undergoing construction and planning. However, there is no clearly defined methodology for such an assessment, although previous studies have been performed, and this work draws on learnings from these.

Although there are examples of wave impact studies for offshore wind developments using phase-resolving mild-slope models, e.g. Cefas (2005), two specific studies have investigated the use of SWAN for such an application. Alari and Raudsepp (2012) addressed the proposed construction of 200 turbines over two sites in northwestern Estonian waters in the Baltic Sea. Running models over 25 m and 50 m resolution bathymetry grids, the authors represented individual turbines in the model as dry grid points rather than barrier structures. Although a 25 m or 50 m dry grid cell is far larger than a typical turbine monopole diameter (5 m), an assumption was made of a linear relationship between the turbine diameter and the calculated differences in wave height. Results for the 25 m grid were therefore divide by 5 (for a 5 m turbine) and by 10 for the 50 m grid. Ponce de Leon et al. (2011) investigated the use of SWAN in more detail, running detailed tests looking at the impact of a single turbine over a very high resolution grid. The turbine monopile was modelled as quasi-circular structure, using a series of angled barriers to construct the monopole shape. However, the model resolution required makes such an approach impossible for a large array of turbines. In order to apply their model to assess the impact of the Norwegian HAVSUL-II offshore wind turbine array, the authors reverted to the same methodology as Alari and Raudsepp (2012), using dry grid cells to represent individual turbines.

2.3 Acoustic Energy Flux sound field model

In comparison with the wave modeling techniques described above the modelled total underwater radiated sound field treats each operational turbines turbine foundation as a potential acoustic source. The acoustic received level at some position in the field is then determined as the sum of all these source terms (acoustic energy at the source). The modelling of sound propagation loss between the individual

turbines and the receiver position is illustrated in Figure 6. Propagation characteristics for a sound field are complex due to surface and seabed interactions and acoustic properties within the water column itself. This is particularly true in shallow water environments (<100 m) where the ability of sound to propagate depends on a wide variety of physical and environmental conditions. The primary dependences rely on properties such as water depth, seabed bathymetry, sediment type, wave height, water column characteristics (sound velocity, density, absorption properties, stratification, etc.). There is also strong frequency dependence where different parts of the sound spectrum will radiate differently in the same environment leading to dispersion effects in the time domain and frequency stripping in the frequency domain (Urick, 1983).

As in the case of operational noise from offshore wind turbine array operation, observations suggests relatively broadband acoustic components with a majority of the contribution in the range of 10's of Hz to around 1 kHz including a series of tonals, (Madsen et al., 2006; Betke et al., 2004). For the present study, to model a broader frequency band, the signal spectrum was segmented into Third Octave Bands (TOB) with centre frequencies at 40, 50, 63, 80, 100, 125, 160, 200, 250, 315, 400, 500, 630, 800 and 1000 Hz. The loss profiles for each band centre frequency were calculated separately. These were then combined with the third octave band source characteristics into individual band-received level profiles radiating out from the source. Finally, the individual received level bands were recombined into the equivalent broadband received level signal. The resultant received level profile is a two dimensional slice of the sound field in the vertical plane of received level in range and depth on a particular bearing from the source. This process can then be replicated many times calculating sound field profiles out to a spatial grid surrounding the source on many bearings. These fields were then combined to interpolate a three-dimensional sound field surrounding the source. A horizontal slice through this can then form a commonly seen plan-view sound map at a particular depth.

Numerous range-dependent numerical sound propagation methodologies exist with varying degrees of accuracy, frequency range and computational power, including Normal-Mode, Parabolic Equation, Wave number integration, Ray tracing etc. (Jensen et al., 1994). Because of the computational intensity of the

number of sources (turbines) (up to 4800 and size of physical environments up to 11804 km^2), a range dependent analytical solution based on Energy Flux Density was used to achieve the many millions of propagation models needed in the scenarios listed in Table 2 in a reasonable time frame. The Energy Flux model developed by (Weston, 1980) and range averaging (Harrison and Harrison, 1995) is a range-dependent solution accounting for bathymetry, sediment type, wind speed and water column properties. The radiated field is then estimated from each source to each point on a spatial grid. The total field contributions from all sources are then estimated at each grid point. Robinson and colleagues ran comparisons of commonly used examples of numerical codes listed above against the energy flux density algorithm, and against empirical data for noise observed from dredging operations in a similar frequency band. They obtained good correlation in shallow water environments, making it ideal for the current application (Robinson et al, 2011).

3 Model scenarios

3.1 Biogeochemical model

An existing GETM-ERSEM-BFM model setup was used for the North Sea, which uses a spherical grid with a spatial resolution of approximately 11 km and 25 layers in the vertical (see www.nioz.nl/northsea_model and also Lenhart et al., 2010). The model was forced with tidal boundary conditions from shelf-scale model, climatological temperature, salinity and nutrient boundary conditions, observations-based river run-off and riverine nutrient loads, and atmospheric forcing from the ECMWF ERA-40 and operational hindcast. A reference run was carried out with the existing model, hot-starting in 1995 from stored states of a 50-year hindcast covering 1958-2008, and running until 2008. Daily values of the main model variables were stored.

The GETM model was modified to allow for the presence of wind turbine arrays through local adjustment of the meteorological forcing. For the scenario results presented here, the wind speed applied to the grid

cells coinciding with the wind turbine array was reduced by 10%, following the reductions reported by Christiansen and Hasager (2005), which were based on satellite observations of a relatively small wind farm in Danish waters. Because of the relatively coarse spatial resolution of the model, within-array detail could not be included here. Wake effects of the wind turbine array on the wind field were not considered, as the wind field typically recovers within 5-20 km of a wind turbine array (Christiansen & Hasager, 2005), a distance comparable to the model grid size. Other potential effects of wind turbine arrays on meteorological forcing and hydrodynamics include changes in air pressure, air temperature and humidity (Roy, 2011), and partial blockage of flow by pilings and an increase in water turbulence introduced by pilings (Rennau et al., 2012). None of these additional effects were considered in this study. In similarity to the reference run, the wind turbine array scenario setup was also run for the years 1995-2008, storing daily values.

The model results of both the reference and the scenario run were depth-integrated, and annual-averaged. Subsequently, the relative difference of the annual averages of the two runs was calculated, and averaged over the years 2005-2008. The results for 1995-2004 were considered to be spin-up, and discarded.

3.2 SWAN

A series of SWAN model runs were performed to enable the impacts of five large-scale offshore wind turbine array scenarios to be predicted. The scale of arrays modelled was based on industry predictions of the potential size of arrays that could be seen in the next fifty years – up to approximately 5000 turbines (The Crown Estate, 2012). In an array of this size, it is probable that turbines will be deployed in individual 'farms', with a wider spacing between farms than between individual turbines to allow for access and navigation across the array. The key question addressed by this modelling study is: what will be the effect of altering the spacing between farms within the larger array, and of altering the size of the farms? A basic array layout was designed, illustrated in Figure 3, comprising four rows of 10 farms, with 5km spacing between farms. Each farm consists of 20 rows of six turbines, spaced 800 m apart. This

gives a total array of 4800 turbines and, assuming each turbine is rated at 5 MW, 24 GW of generating capacity.

The physical size of the array requires a SWAN grid representing a geographical domain of 89 x 77.6 km, defined with a resolution of 100m to satisfy the available computational resources.

In addition to the basic array layout, four further array scenarios were designed to test the impact of farm spacing and size. In scenarios 2 and 5, the number of turbines was halved to keep the footprint of the array approximately the same size while increasing farm spacing, while in scenarios 3 and 4 the array footprint was increased substantially. The details of the five array scenarios are presented in Table 2. Each turbine was represented in the model as a dry grid point, following the recommendations of Alari and Raudsepp (2012) and Ponce de Leon et al. (2011). In SWAN, land absorbs all incoming energy so there will be no reflection, only diffraction, of the incident wave.

The model bathymetry was set to a constant water depth of 20m, typical of offshore wind sites. All default SWAN settings for energy generation and dissipation and wave-wave interaction processes were used, as described by the SWAN Team (2006), and diffraction was activated. Quadruplet interactions were de-activated unless wind input was used in a particular model run. Examination of a scatter diagram from a wave buoy deployed at Dogger Bank in the North Sea, typical of an offshore deployment site, shows the most frequently occurring wave states have a significant wave height H_s in the range of 1.5 – 2 m and mean wave period (T_z) 3 – 6 s (Table 3). As the data were recorded from January to August and therefore exclude autumn storm conditions, a sea state from the upper end of this range (H_s = 2 m, T_z = 6 s) was selected as input for the model. This sea state was input along the southern boundary of the model. The model was initially run with no turbines included to predict the baseline H_s at each location. This was followed by model runs for each of the five array scenarios, and the percentage difference in H_s, ΔH_s, was calculated at each grid point Using Alari and Raudsepp's (2012) assumption of linear dependence between the diameter of the turbine and the change in wave height, and based on a hypothetical 10 m diameter turbine pile, these results for ΔH_s were divided by 10 to reflect the 100m grid resolution. This assumption can only be avoided by resolving the turbines using a finer grid, which on the spatial scale of

the farms considered here substantially exceeded the available computational resource. The current results can easily be re-scaled with an alternative linear relationship.

The effects of wind on the results were also investigated using the scenario 1 layout and various settings for wind speed and direction.

3.3 Acoustic Energy Flux sound field model

Although there has been significant growth in concern of potential adverse impacts of underwater noise on the marine environment over the last couple of decades, (Richardson et al., 1995), there is currently little data in the public domain on the source-characteristics of operational windfarms. Especially potential impacts from large-scale up-scaling such as the scenarios envisaged in this study are worth considering.

A number of studies have been completed. Madsen et al. (2006) reported third octave band-received levels for centre frequencies from 20 Hz to 1 kHz at at range of 83 m from an operational turbine at wind speeds of 8 and 13 ms^{-1}. Similarly Betke et al. (2004) reported received levels at a range of 110 m from a 1500 kW turbine at 17 and 12 ms^{-1}, and from an 80 kW turbine at 3.5 ms^{-1}. Both studies show individual TOB band-received levels in excess of 110 dB referenced to 1 µPa (RMS) at higher wind speeds. Other data on large turbines has been measured but is currently not in public domain. In the absence of empirical evidence of causal links between noise levels and turbine size (power), the data from these studies is used as a proxy for the larger turbines (5 MW) envisaged in this study. Third octave bands with centre frequencies between 10 Hz and 1 kHz were modelled using source data per band based on the Betke and Madsen et al studies with an equivalent broadband source level energy of 167.6 dB re 1µPa-m (RMS).

Several specfic case studies were developed to investigate the effect of large scale up-scaling the interaction of multiple turbine operation within a farm. Figure 7 shows the most south-westerly farm layout and depth bathymetry and near neighbours as outlined in scenario 1 (Figure 3, Table 2). As with

previous studies all models were run under identical conditions using common source characteristics, sediment types, oceanographic data, etc. The seabed was assumed to be a homogenous sand layer with a compressional sound velocity 1628 ms^{-1}, density of 1900 kgm^{-3}, and compressional absorption of 0.8 dB per wavelength (Hamilton, 1980) and a uniform sound velocity of 1480 ms^{-1} was assumed in the water column.

This south-westerly wind farm shows a relatively large variation in water depth (45-50 m to around 25 m from the south to the north of the site). Other specific farms and neighbours were also modelled across the scenario 1 layout with a 5 km spacing between farms, including the most north-eastly farm which lies in much more uniform depth of around 25-30 m. Comparison was also made with scenario 2 farm to farm interactions where adjacent east-west farms are located 10 km apart.

4 Results and Discussion

4.1 Biogeochemical model

The results show (Figure 1, Table 1) a reduction in wave height within the area of the wind turbine array of 17%, leading to a reduction in suspended sediment concentrations of 25% and a reduction in light extinction of about 17%. This led to an increase in net primary production of about 8%, with an associated reduction in nitrate concentrations of 6% and a 3% increase in chlorophyll concentration. Gross secondary production increased by about 10%. TEP concentrations increased by 17%. This led to increased sinking of particulate material, resulting in an increase of 35% and 20% in phytoplankton and zooplankton food supply to benthic suspension feeders. As a result, suspension feeder biomass increased by 13% in the area of the wind turbine array, but also showed reductions of about 5% to the north and south of the array area. Overall, the benthic carbon content within the array area increased by 15%. The model run including the operational threshold of 25 m/s showed only minor differences (Table 1). Time series of net primary production and nitrate concentrations at the surface in the centre of the wind farm

(Figure 2) shows that the main differences are caused by an earlier onset of the spring bloom because of the improved light conditions leading to an earlier draw-down of nutrients at the expense of slightly later production, and also by a slight increase in production at the end of the growing season, leading to a delay in the recovery of winter nutrient concentrations.

The ecosystem model results suggested that the presence of an operational wind turbine array will lead to a general increase in ecosystem productivity in the array area. Pelagic effects were mostly limited to the location of the wind turbine array, whereas benthic effects occurred in a radius of about two array cross-sections. These results may be related to the particular location of the array, which was in an area of weak currents. An array in an area with stronger currents might lead to stronger far-field effects. If this were the case, and if multiple arrays were introduced, inter-array interaction might occur.

The limited changes in chlorophyll concentrations as opposed to those in net primary production are attributed to grazing by zooplankton, leading to the increased secondary production. The reduction in nutrient concentrations in the array area led to increased TEP production by diatoms, which resulted in increased coagulation and sinking rates, and led to increased food supply to the benthic suspension feeders, fuelling benthic productivity, and increasing the local carbon content of the sea bed. Introducing a 25 m/s (10 Beaufort) threshold wind speed for the operation of the array resulted in only minor differences, presumably because such events are relatively rare and of short duration.

If the influence of the turbine support structures on the hydrodynamics were included, an increase in turbulence might be expected, which would lead to an increase in turbidity. Such a process would counteract, and might even reverse, the effects reported on here. Modeling these effects would require a much more sophisticated SPM model than used here (e.g., such as reported by van der Molen et al., 2009). Hence, the modelled response reported here is likely to be an overestimate.

If the presence of a wind turbine array at sea would lead to an increase in local air temperature similar to that reported for a wind farm located on land (Roy, 2011), one might expect local effects mimicking those of climate change. Climate change effects were studied with a 1D water-column version of the current

model (van der Molen et al., 2013), suggesting increased primary production and increased pelagic recycling rates, the latter leading to a reduction in food supply to the benthic system and reduced benthic biomass. Such a response to an increase in temperature would amplify the increase in pelagic primary and secondary production reported here, and would also dampen the increase in benthic biomass.

4.2 SWAN

The calculated reduction in H_s across the array for scenario 1, the basic array layout, is shown in Figure 4. It illustrates how the impacts increase with distance through the grid. Although the largest reductions in H_s are found within the individual farms, the effect of wave spreading means that the impact in the inter-farm spacing becomes almost as significant towards the furthest extremes of the array. For each of the scenarios, the average and maximum percentage reduction in H_s across the domain were calculated. The results, presented in Table 4, illustrate the effect of farm size and spacing within the larger array. The largest average reduction in H_s (5.87%, with a maximum reduction of 9.58%) occurred for the baseline scenario 1, with 40 farms of 120 turbines spaced 5km apart. Halving the size of the array to 20 farms in scenario 2, but keeping the same spacing as scenario 1 produced the lowest reductions in H_s (average 4.3%, maximum 8.62%). Increasing the east-west separation to 10km in scenario 3 decreased the average wave height reduction to 4.51%, although the maximum reduction remained close to that for scenario 1 at 9.23%. The largest reduction, 9.65%, was found in scenario 4 when farms of 12 x 20 turbines were modeled. Decreasing the farm size to 3 x 20 turbines in scenario 5 did not produce a notable decrease in the overall wave height reduction.

The results from the investigation into the effects of wind are presented in Table 5. Model runs were performed for three wind speeds (5 ms^{-1}, 10 ms^{-1} and 20 ms^{-1}) from the south, aligned with the mean wave direction. A reduction of 10% in wind speed from 10ms^{-1} to 9ms^{-1} to simulate an instance of the 10% reduction used in the ecological model was also tested. Finally, a model run with a 10ms^{-1} westerly wind was performed to test the effect of wind direction. All model runs used the scenario 1 array layout. The

results over the grid domain for the 10ms^{-1} southerly wind are illustrated in Figure 5. When comparing these results to the model run with no wind (Figure 4), it becomes clear that in addition to reducing the average and maximum reductions in H_s, the main effect of the wind is an increased consistency in the impact on wave height across the array. This is because the wind is transferring energy to the waves between turbines and farms, so the effects do not reinforce themselves across the whole grid as shown in Figure 4.

The model runs completed with no wind provide an indication of the importance of array layout and farm spacing. In general, larger spacing between farms leads to lower average and maximum reductions in wave height, as does fewer turbines in the sub-farms. However, these differences are only in the region of 1.5%, and are small compared to the effects of including wind in the model. There will rarely be negligible wind at an offshore wind turbine array, so the inclusion of wind is of key importance to this assessment. A series of model runs with different wind scenarios was carried out. Only summary numerical results are provided (Table 5), because the spatial patterns generated by these runs were similar to those presented so far. Although a light wind of 5 ms^{-1} has little impact on the results, increasing this to 10ms^{-1} begins to show a notable contribution in re-generating waves within the array, with the average reduction in wave height reduced by over 1.5%. A far more consistent reduction across the array is also seen as energy is continually transferred to the waves, in contrast to the progressively larger effect through the array seen with no wind included. Larger wind speeds of 20 ms^{-1} see the average wave height reduction more than halved. The wind direction appears to play only a small role in influencing the results, with energy transferred to the waves regardless of the direction. Although not investigated in this study, the main impact of wind direction is likely to be on the direction of the waves rather than their height. When a realistic reduction in wind speed of 10% (i.e. 10 ms^{-1} to 9 ms^{-1}) is applied across the array to represent energy extraction by the turbines, a slight increase in the impact can be seen, but this is small compared with the effect of including wind speed.

Most of the model scenarios presented in the study have focused on the intra-array impacts. However far-field effects are also of importance, particularly when considering the ecological modeling described in section3.1. To investigate this issue, two further model runs were performed for Scenario 1, with the northern model boundary extended by 30 km. The first run, with no wind included, predicted a reduction in wave height of 4.75% could still be seen at a distance of over 30km from the last row of turbines. When a 10 ms^{-1} southerly wind was included, this reduced to 1.64%, implying that in a realistic scenario, far-field effects are unlikely to be of major significance.

It should be noted that this methodology provides a simplistic approach to the modelling of offshore wind turbine arrays. Effects such as wave reflection from turbine piles are ignored, as are the complex hydrodynamic wave interactions that would occur in the immediate wake of the pile. The necessary use of the 100m resolution grid also requires an assumption to be made of the linear dependence between turbine diameter and wave height reduction. However, this methodology allows much larger arrays to be modeled than could otherwise be addressed, and provides valuable insights into the potential impacts of such large-scale developments.

4.3 Acoustic Energy Flux sound field model

Figure 8 shows the computed broadband sound field for the most south westerly wind farm selected from scenario 1. The individual turbines have a broadband (~40-1000 Hz) source level of 167.6 dB re 1 µPa-m (RMS). Across the site broadband levels quickly (within a few hundreds of meters) drop to broadband levels less than 120 dB re 1 µPa (RMS). This happens more rapidly in the deeper water (40-45 m) to the south of the farm. To the north a sharp incline is seen in the bathymetry up to a plateau of around 25 m. In the shallower water the sound field propgates slightly better allowing a slightly broader spread seen on indvividual turbines in the north of the farm. This correlation of improved propagation at 25 m depth is also reflected in the easterly neighbour where the shallow water extends further down the farm.

Looking at the mid points between two turbines at 800 m spacing, Figure 8 shows the minimum broadband level within the farm is around 113 dB re 1 µPa (RMS) throughout the farm, compareable with levels of below 113 dB within 400 m of the farm to the west. To the east farm to farm interaction can be seen with levels bottoming out at around 102 dB re 1 µPa (RMS). Again outside the whole scenario envelope levels drop below these minimium levels within a few hundred meters. Figure 9 shows the east-west profile for the 16th row of the two lower farms (shown in Figure 8 as a dotted line). The minimium level within the farm dropping to around 53 dB below the individual turbine source level. Similarly the farm to farm spacing in scenario 1 of 5 km is 10 dB lower at 63 dB below the individual turbine source level. These differences are relatively consistent across the farm due to the relative evenness of the bathymetry seen across the whole scenario. The difference due to the propagation conditions seen from the north to the south of the farm makes around a 2 dB in minimum levels (greatest distance from the pile but within the farm) with levels of around 115 dB re 1 µPa (RMS) seen in the shallower water (more typical across rest of the scenario). Similarly in the profile shown in Figure 9 the minimium levels within the easterly farm are around 2 dB higher around 115 dB re 1 µPa (RMS) due to the local propgation conditions.

Figure 9 shows the farm to farm level dropping to around 102 dB re 1 µPa (RMS) between the two farms. This can be compared with a scenario 2 model (shown in Figure 10): again for the south-westerly corner of the whole array. The first farm is an identical grid of 6 x 20 turbines, however in this case a10 km spacing is introduced. In this case minimum levels between the farms may drop slightly lower with potential for levels less than 100 dB re 1 µPa (RMS). This potential contribution to large areas for very large arrays can be seen in Figure 11. This model includes 2400 turbines modeled with 60 turbines per farm in a 3 x 20 grid with 5 km farm to farm spacing (scenario 5, Table 2). In this case the relatively uniform bathymetry results in minimium levels in the farm of around 113-115 dB re 1 µPa (RMS) and within the total array of 102 dB re 1 µPa (RMS) over an area greater than 46,00 km^2. Again the effects of the slightly deeper water to the south of the most south westerly farm can be seen as well as changes in farm to fram levels in from the South to the North of the whole array on the Eastern farms. Because of the

size of these modelled scenarios potential noise contributions exist over significant areas of ocean with higher areas within the farms and directly localized on the turbines themselves. Contributions between turbines and farm to farm should however be considered carfully in context of relatively high ambient noise seen on these sites and other distant and local noise sources discussed further in the following section. Note that in all these modelled levels we assume coherent summation from multiple sources either as turbine to turbine interaction or farm to farm, and as such these represent a worst case stable constructive / destructive interferences scenario. In reality a strong phase coherence is unlikely and therefore generated fields will likely exhibit lower average levels than the spatially stable interference fields modelled here.

In the context of array design and configuration, slight increases of within-farm noise levels are seen in shallower water with potential for cumulative effects from both turbine to turbine and farm to farm. This however should be compared to other local noise sources directly related to the windfarm operation such as nearby maintenance vessels.

These minimum introduced levels in between two farms and even within a farm may under certain sea-states be below typical broadband ambient-noise levels observed in common windfarm sites. As a result outside individual farms and the whole array the introduced noise level is likely to be below that of existing ambient noise at relatively short ranges from the outermost turbines for a proportion of or the whole of the radiated noise spectrum.

For ambient noise levels greater than 102 dB re 1 μPa (RMS), for example farm to farm sound levels at short distance outside the farm will be identical to levels a short distance outside the entire array envelope. Similarly within the farm ambient noise levels may often exceed the equivilent turbine to turbine interaction levels as illistated in Figure 8. Increased turbine noise as a function of wind-speed and sea-state will also be associated with increases in ambient noise levels (Urick, 1983). Overall, perception-wise, individual turbines are likely to be detectable for a range of marine species but at relatively short rangesMany common UK cetacean and pinniped species have optimized hearing at frequencies well

above those of the radiated noise spectrum however many retain hearing capabilities within this band making detection a possibility. For many fish species and larger marine mammals this band overlaps significantly with peak hearing response, (Ainslie, 2010; Nedwell et al., 2004). Under low ambient-noise conditions multiple turbines may be detectable, but likely to occur for lower wind speeds and therefore potentially lower noise output.

Regardless of perception, individual farms and much larger arrays of farms as seen in the modeled scenarios of many thousands of turbines do offer potential to make relatively small (a few dB) increases in average ambient noise levels over large areas of ocean for extended periods of time. The relative importance of this combined with other anthropogenic noise sources to the marine habitat is unknown at this time.

5 Concluding remarks

The results of the wave model suggest substantial repetitive spatial variability in the changes in wave height, related directly to the layout of the array. A similar argument holds for the noise model. The ecosystem model does not resolve these spatial scales, but it may be expected that, if the ecosystem response as simulated at the array scale carries over to smaller scales, the ecosystem response to a real array may also result in repeating spatial variations. This could lead to a larger spatial heterogeneity in ecosystem characteristics (disregarding the presence of the hard structures introduced by the turbine foundations) than would be present in absence of the wind turbine array. However, because of temporal variations in wind speed and direction (not included in the wave model), and because of the increased importance of advection and diffusion of pelagic ecosystem components at the within-array and farm scale as compared to the array scale and larger considered in the ecosystem model, it may be expected that such spatial heterogeneity in ecosystem characteristics would be less pronounced than the patterns suggested by either the wave- or the acoustic-model results.

Further considering spatial scales, the acoustic model suggests that, compared with effects on waves and the ecosystem, the noise footprint of individual turbines is the most concentrated. The footprint of the ecosystem effects is likely to be the most diffuse, because advection with currents is likely to play a role which is less important for surface waves.

The results of the wave model suggest that the reduction in wave height simulated by the ecosystem model is over-estimated by more than a factor of 2. Hence, the impacts on the ecosystem of a real array may well be less than suggested by the current ecosystem model simulations.

The functional types included in the ecosystem model are at low trophic levels in the food chain, which are not expected to respond to noise. Rather, they would present a food source for higher trophic levels, some of which can be expected to respond to noise. If the increased productivity within the array as indicated by the ecosystem model is not negated by other effects not included in this study (see section3.1), then a wind turbine array will present an area with slightly increased food levels, potentially of higher variety than in the surrounding areas, and slightly quieter wave conditions, but at slightly higher noise levels and with obstructions, to fish, mammals and sea birds. So in absence of other disturbing factors, and depending on species-specific characteristics and preferences, wind turbine arrays are likely to present a weak attraction (increased levels of food, reduced sea state) and a weak repulsion (noise). Given the different gradients of noise, sea state and expected ecosystem effect as a function of distance from the individual turbines, a variety of combinations of these factors is likely to exist within a wind turbine array, potentially allowing species sensitive to these forcings to select the most favourable ones. Other factors, not modelled here, may come into play as well, such as hazard (obstacles) and orientation (visual and acoustic elements in an otherwise featureless sea).

Overall, the results of this initial study suggest that, in response to the forcings and mechanisms included here (which cover only a subset of the potential effects, and were mostly modelled separately, thus excluding interactions), and subject to the assumptions made (which include substantial uncertainty in the effects of large-scale arrays on surface winds), the impacts of large-scale wind turbine arrays on the marine ecosystem may be relatively minor. Also, and rather unsurprisingly, they suggest that the effects

decrease with increasing distance between (groups of) turbines, which suggests that fewer, more powerful turbines may introduce less impact than a larger number of lighter ones. Further work is required to include additional forcings, mechanisms and effects that were disregarded here (SPM transport, wave propagation in the ecosystem model, wakes, turbulence induced by structures, additional SPM resuspension induced by this additional turbulence, reflection of waves on the structures, operational noise as a function of turbine size, attachment of organisms to structures, higher trophic levels, etc.). Moreover, observations of all these effects in and around real wind turbine arrays are required to test and validate these models.

Acknowledgements

The work was carried out as part of the EBAO project (Optimising Array Form for Energy Extraction and Environmental Benefit), and was jointly funded by NERC and Defra (Cefas contract C5325).
Sonja van Leeuwen constructed the daily riverine loads database from which the runoff data were used in the GETM-ERSEM model. French water quality data were supplied by the Agence de l'eau Loire-Bretagne, Agence de l'eau Seine-Normandie and IFREMER. UK water quality data were processed from raw data provided by the Environment Agency, the Scottish Environment Protection Agency and the National River Flow Archive. The German river loads are based on data from the ARGE Elbe, the Niedersächsisches Landesamt für Ökologie and the Bundesanstalt für Gewässerkunde. The river load data for the Netherlands were supplied by the DONAR database.
The authors gratefully acknowledge the ECMWF (European Centre for Medium Range Weather Forecasting) for allowing the use of the ERA-40 and Operational Hindcast data used as atmospheric forcing for the GETM-ERSEM model.

References

Alari, V., Raudsepp, V., 2012. Simulation of wave damping near coast due to offshore wave farms. J. Coast. Res. 28 (1), 143-148.

Ainslie, M. A., 2010. Principles of Sonar Performance Modelling, Springer, Berlin, Heidelberg.

Baretta, J.W., Ebenhöh, W., Ruardij, P., 1995. The European Regional Seas Ecosystem Model, a complex marine ecosystem model. J. Sea Res. 33, 233-246.

Betke, K., Schlutz-von Glahn, M., Matuschek, R., 2004. Underwater noise emmissions from offshore wind turbines. Proceedings CFA/DAGA'04, 1-2.

Booij, N., Ris, R.C., Holthuijsen, L.H., 1999. A third-generation wave model for coast regions, Part 1, model description and validation. J. Geophys. Res., 104 (C4), 7649-7666.

Burchard, H., Bolding, K., 2002. GETM – a general estuarine transport model. Scientific documentation, Tech. Rep. EUR 20253 EN, European Commission.

Cefas, 2005. Assessment of the significance of changes to the inshore wave regime as a consequence of an offshore wind array. Cefas, Lowestoft, UK.

Christiansen, M.B., Hasager, C.B., 2005. Wake effects of large offshore wind farms identified from satellite SAR. Rem. Sens. of Env. 98, 251 – 268.

Engel, A., 2000. The role of transparent exopolymer particles (TEP) in the increase in apparent particle stickiness (α) during the decline of a diatom bloom. J. Plankt. Res. 22(3), 485-497.

EU, 2009. EU Directive 2009/28/EC of the European Parliament and of the Council of 23 April 2009 on the promotion of the use of energy from renewable sources and amending and subsequently repealing Directives 2001/77/EC and 2003/30/EC (Text with EEA relevance).

Fayram, A.H.; Risi, A., 2007. The Potential Compatibility of Offshore Wind Power and Fisheries: An Example using Bluefin Tuna in the Adriatic Sea. Ocean Coast. Man., 50(8), 597-605.

Gill, A.B., 2005. Offshore renewable energy - ecological implications of generating electricityin the coastal zone. J. App. Ecol., 42, 605-615.

Grainger, B., Thorogood, T., 2001. Beyond the harbour wall. IEE Review 47, 13-17. DOI: 10.1049/ir:20010202.

Hamilton, E.L., 1980. Geoacoustic modelling of the sea floor. J. Acoust. Soc. Am. 68(5), 1313-1340.

Harrison, C.H., Harrison, J.A., 1995. A simple relationship between frequency and range averages for broadband sonar. J. Acoust. Soc. Am. 97(2), 1314-1317.

Holthuijsen, L.H., Herman, A., Booij, N., 2003. Phase-decoupled refraction diffraction for spectral wave models. J. Coast. Eng. 49, 291-305.

Inger, R., Attrill, M.J., Bearhop, S., Broderick, A.C., Grecian, W.J., Hodgson, D.J., Mills, C., Sheehan, E., Votier, S.C., Witt, M.J., Godley, B.J., 2009. Marine renewable energy: potential benefits to biodiversity? An urgent call for research. J. App. Ecol., 46, 1145-1153.

Jensen, F.B, Kuperman, W.A., Porter, M.B, Schmidt, H., 1994. Computational Ocean Acoustics. New York, American Institute of Physics. ISBN: 1563962098.

Langhamer, O., Wilhelmsson, D., 2009. Colonisation of fish and crabs of wave energy foundations and the effects of manufactured holes - a field experiment. Mar. Env. Res. 68(4), 151-157.

Lenhart, H.J., Mills, D.K., Baretta-Bekker, H., van Leeuwen, S.M., van der Molen, J., Baretta, J.W., Blaas, M., Desmit, X., Kühn, W., Lacroix, G., Los, H.J., Ménesguen, A., Neves, R., Proctor, R., Ruardij, P., Skogen, M.D., Vanhoutte-Grunier, A., Villars, M.T., Wakelin, S.L., 2010. Predicting the consequences of nutrient reduction on the eutrophication status of the North Sea. J. Mar. Syst. 81, 148-170.

Linnane, A., Mazzoni, D. and Mercer, J. P., 2000. A long term mesocosm study on the settlement and survival of juvenile European lobster *Homarus gammarus* in four natural substrata. J. Exp. Mar. Biol. Ecol. 249, 51-64.

Madsen, P.T., Wahlberg, M., Tougaard, J., Lucke, K., Tyack, P., 2006. Wind turbine underwater noise and marine mammals: implications of current knowledge and data needs. Mar. Ecol. Progress Series 309, 279-295, doi:10.3354/meps309279.

Millar, D.L., Smith, H.C.M., Reeve, D.E., 2007. Modelling analysis of the sensitivity of shoreline change to a wave farm. Oc. Eng. 34, 884-901, DOI: 10.1016/j.oceaneng.2005.12.014.

Nedwell, J.R., Edwards, B., Turnpenny, A.W.H., Gordon, J. (2004). Fish and Marine Mammal Audiograms: A summary of available information, Subacoustech Ltd, Report ref: 534R0214. 281.

Neill, S.P., Litt, E.J., Couch, S.J., Davies, A.G., 2009. The impact of tidal stream turbines on large-scale sediment dynamics. Ren. En., 34(12), 2803-2812. doi:10.1016/j.renene.2009.06.015.

Offshore Energy Strategic Environmental Assessment 2 (OESEA2), 2011. Post public consultation report. Department of Energy & Climate Change, https://www.gov.uk/government/uploads/system/uploads/attachment_data/file/197708/OESEA2_Post_Consultation_Report.pdf, 69pp.

OSPAR, 2008. Assessment of the environmental impact of offshore wind-farms. OSPAR Comm. Publ. 385/2008, ISBN 978-1-906840-07-5.

Peperzak, L., Colijn, F., Gieskes, W.W.C., Peeters, J.C.H., 1998. Development of the diatom-Phaeocystis spring bloom in the Dutch coastal zone of the North Sea: the silicon depletion versus the daily irradiance threshold hypothesis. J. Plankt. Res. 20(3), 517-537.

Petersen, J.K., Malm, T., 2006. Offshore Windmill Farms: Threats to or Possibilities for the Marine Environment. AMBIO: A Journal of the Human Environment, 35(2), 75-80.

Ponce de Leon, S., Bettencourt, J.H., Kjerstad, N., 2011. Simulation of irregular waves in an offshore wind farm with a spectral wave model. Cont. Shelf Res. 31, 1541-1557. DOI: 10.1016/j.csr.2011.07.003.

Radach, G., Moll, A., 2006. Review of three-dimensional ecological modelling related to the North Sea shelf system. Part II: Model validation and data needs. Oceanogr. Mar. Biol.: An Annual Review 44, 1-60.

Rennau, H., Schimmels, S., Burchard, H., 2012. On the effect of structure-induced resistance and mixing on inflows into the Baltic Sea: A numerical model study. Coast. Eng. 60, 53–68.

Richardson, W.J., Greene, C.R. Jr., Malme, C.I., Thomson, D.H., 1995. Marine Mammals and Noise, Academic Press.

Robinson, S.P., Theobald, P.D., Hayman, G., Wang, L.S. Lepper, P.A., Humphrey, V., Mumford, S., 2011. Measurement of noise arising from marine aggregate dredging operations. MALSF. ISBN 978 0907545 57 6.

Roy, S.B., 2011. Simulating impacts of wind farms on local hydrometeorology. J. Wind Eng. Ind. Aerodyn. 99, 491–498.

Ruardij, P., van Haren, H., Ridderinkhof, H., 1997. The impact of thermal stratification on phytoplankton and nutrient dynamics in shelf seas: a model study. J. Sea Res. 38, 311-331.

Ruardij, P., van Raaphorst, W., 1995. Benthic nutrient regeneration in the ERSEM-BFM ecosystem model of the North Sea. Neth. J. Sea Res. 33, 453-483.

Ruardij, P., Veldhuis, M.J.W., Brussaard, C.P.D., 2005. Modeling the bloom dynamics of the polymorphic phytoplankter *Phaeocystis globosa:* impact of grazers and viruses. Harmf. Alg. 4, 941-963.

Rusu, E., Guedes Soares, C., 2013. Coastal impact induced by a Pelamis wave farm operating in the Portuguese nearshore. Renew. En. 58, 34-49, DOI: 10.1016/j.renene.2013.03.001.

Skogen, M.D., Moll, A., 2005. Importance of ocean circulation in ecological modelling: An example from the North Sea. J. Mar. Syst. 57, 289-300.

Smith, H.C.M., Pearce, C., Millar, D.L., 2012. Further analysis of change in nearshore wave climate due to an offshore wave farm: An enhanced case study for the Wave Hub site. Renew. En. 40, 51-64.

SWAN Team, 2006. SWAN User Manual. Delft University of Technology, Delft, 137 pp.

The Crown Estate, 2012. UK offshore wind report 2012. The Crown Estate, London, 12 pp., www.thecrownestate.co.uk/media/297872/UK%20offshore%20wind%20report%202012.pdf.

Urick, R.J., 1983. Principles of underwater sound, 3rd Edition, McGraw-Hill, New York, ISBN 0070660875.

van der Molen, J., Aldridge, J.N., Coughlan, C., Parker, E.R., Stephens, D., Ruardij, P., 2013. Modelling marine ecosystem response to climate change and trawling in the North Sea. Biogeochem. 113, 213-236, DOI 10.1007/s10533-012-9763-7.

Van der Molen, J., Bolding, K., Greenwood, N., Mills, D.K., 2009. A 1-D vertical multiple grain size model of suspended particulate matter in combined currents and waves in shelf seas. J. Geophys. Res. 114, F01030, doi:10.1029/2008JF001150.

Van Rijn, L.C., 1994. Principles of fluid flow and surface waves in rivers, estuaries, seas and oceans. Aqua Publications, Oldemarkt, 2nd Edition , ISBN 90-800356-1-0.

Vichi, M., May, W., Navarra, A., 2003. Response of a complex ecosystem model of the northern Adriatic Sea to a regional climate change scenario. Clim. Res. 24, 141-158.

Vichi, M., Pinardi, N., Masina, S., 2007. A generalized model of pelagic biogeochemistry for the global ocean ecosystem. Part I: Theory. J. Mar. Syst. 64, 89-109.

Vichi, M., Ruardij, P., Baretta, J.W., 2004. Link or sink: a modelling interpretation of the open Baltic biogeochemistry. Biogeosci. 1, 79-100. SRef-ID: 1726-4189/bg/2004-1-79.

Weston, D.E., 1980. Acoustic flux methods for oceanic guided waves. J. Acoust. Soc. Am. 68 (1), 287-296, doi: dx.doi.org/10.1121/1.384592.

Wilhelmsson, D., Malm, T., Ohman, M.C., 2006. The influence of offshore wind power on demersal fish. ICES J. Mar. Sci., 65(5), 775-784.

Wilson, JC, Elliott, M., 2009. The potential for habitat creation produced by offshore wind farms. Wind En., 12: 203-212.

Appendix A. A wave shear stress related SPM formulation

SPM concentrations in the ecosystem model were calculated as follows:

The percentage of silt in bottom based on porosity is:

$$S_p = \frac{\varepsilon - \varepsilon_0}{c_1} \qquad (1)$$

where ε is sea bed porosity, ε_0=0.38662 is the porosity for a pure sand bed, and c_1=0.00415 an empirical constant (Ruardij, pers. comm., 2007).

Turn this percentage into a relative number between 0 and 1, and apply a limiting minimum. The minimum was introduced to allow for a minimum background concentration of SPM, depending on depth and wave characteristics, even in absense of silt in the bed to obtain finite concentrations of material in areas where it would be transported through, but never settle into the bed. The relative concentration is then

$$S_r = \max\left(S_0, \frac{S_p}{100}\right) \qquad (2)$$

with S_0=0.3 the limiting mimimum (tuning parameter).

The H_s and zero-crossing period from the equilibrium formulation for fully developed waves were based on the JONSWAP spectrum (van Rijn, 1994, p. 331):

$$H_s = c_2 \frac{U^2}{g} \quad (3)$$

$$T_z = c_3 \frac{U}{g} \quad (4)$$

with g gravitational acceleration, c_2=0.243 and c_3=8.14 empirical constants and U an adjusted wind speed:

$$U = c_4 W^{c_5} \quad (5)$$

with W the local wind speed at 10 m above the surface, and c_4=0.7 and c_5=1.2 empirical constants.

For wave height, a minimum value H_0=0.75 m was assumed to ensure a background hydrodynamic activity that can generate SPM concentrations even in windless conditions, to account for e.g. far-field waves travelling into the area and/or tidal currents:

$$H_s = \max(H_0, H_s) \quad (6)$$

Limitation of wave height in shallow water due to wave breaking follows from:

$$H_s = \min(0.4h, H_s) \quad (7)$$

with h local water depth.

For (zero-crossing) wave period, a minimum of $T_{z,0}$ = 5 s was assumed to be a reasonable minimum for coastal conditions with low wind speed. Effectively, this rule keeps the orbital velocity calculation (9) finite.

$$T_z = \max\left(T_{z,0}, T_z\right) \quad (8)$$

The wave-orbital velocity amplitude at the sea bed was calculated using linear wave theory:

$$u_w = \frac{\pi H_s}{T_z \sinh\left(\frac{2\pi}{T_z}\sqrt{\frac{h}{g}}\right)} \quad (9)$$

The wave-induced bed-shear stress then followed from:

$$\tau_w = \tfrac{1}{2} f_w \rho u_w^2 \quad (10)$$

where ρ is water density and f_w=0.1 a wave-friction factor.

The SPM concentration C_s at the surface that would have occurred if the suspended material present at the previous time step C^{k-1} would be allowed to settle was calculated using an exponential decay formulation as:

$$C_s = C^{k-1} e^{-K_{td}\Delta t} \quad (11)$$

where k is the current time step number, and Δt the model time step in seconds. The decay time scale K_{td} was defined as a function of the surface concentration to simulate that coarse fractions settle faster than fine fractions:

$$K_{td} = \max\left(0, c_{60} + c_{61} C^{k-1}\right) \quad (12)$$

with c_{60}=-0.02/(24*3600) ensuring a background concentration, and c_{61}=8.0/(24*3600) a proportionality constant to set the concentration dependence.

The potential new SPM surface concentration was calculated to be proportional to the shear stress:

$$C_p = c_7 S_r \tau_w \quad (13)$$

with c_7=100.0 a tuning parameter that sets the magnitude of the SPM concentration in response to an applied bed-shear stress.

The new SPM surface concentration was calculated as the maximum of the settling and stirring concentration

$$C^k = \max\left(C_s, C_p\right) \quad (14)$$

The SPM bottom concentration was assumed to be 10 times the surface concentration, with a linear profile to the surface. For locations with a pycnocline, concentrations above the pycnocline were set to zero.

Captions

Table 1. Percentage change of key physical and ecosystem variables for all scenario's considered in GETM-ERSEM-BFM.

Table 2. Array and farm layouts for the five scenarios to be modelled

Table 3. Scatter diagram from a North Sea wave buoy, recorded January – August 2010, with the most frequently occurring sea states highlighted by the red ellipse.

Table 4. Average and maximum reductions in significant wave height for the modeled scenarios from SWAN.

Table 5. Average and maximum reductions in significant wave height for variable wind conditions using the baseline array layout from scenario 1 from SWAN.

Figure 1. 4-year average of relative differences between the reference run (no wind turbine array) and the scenario run for a range of pelagic and benthic variables from GETM-ERSEM-BFM. The black rectangle marks the wind turbine array area. The printed percentage is the average over the wind turbine array area.

Figure 2. Time series of a) net primary production (netPP) and b) nitrate (N3n) at the surface at the centre of the wind turbine array (54.7°N, 1.85°E) for the reference and wind farm scenario from GETM-ERSEM-BFM.

Figure 3. Basic farm design (Scenario 1) for modelling the effects of a large-scale wind turbine array

Figure 4. Percentage reduction in significant wave height due to scenario1 array layout from SWAN.

Figure 5. Percentage reduction in significant wave height due to scenario1 array layout with a constant 10ms^{-1} southerly wind across the domain from SWAN.

Figure 6. Energy Flux model (Weston, 1976) sound field model. At each receiver point the predicted sound field is the arithmetic sum of the depth averaged total energy contributions from each of the sources arriving at that point.

Figure 7. Layout and bathymetry of the most south-westerly farm and near neighbors taken from scenario 1. Crosses and circles represent individual turbine locations.

Figure 8. Broadband (40 Hz-1 kHz TOB's) depth averaged sound field (SPL) from most south-westerly farm and near neighbors from scenario 1, table 2, from the sound field model.

Figure 9. Broadband received level (SPL) west-east profile passing through the 16th row (from southern end) of the most south-westerly farm modeled in scenario 1, from the sound field model.

Figure 10. Broadband (40 Hz-1 kHz TOB's) depth averaged sound field (SPL) from most south-westerly farm and near neighbors from scenario 2, from the sound field model.

Figure 11. Broadband (40 Hz-1 kHz TOB's) depth averaged sound field (SPL) 2400 turbine array arranged from 40 x 60 turbine farms with a farm to farm spacing of 5 km (scenario 5, table 2, from the sound field model).

Tables

Table 1

	10% reduction	10% reduction below 25 m/s
Significant wave height	-17	-17
Suspended sediment	-25	-25
Extinction coefficient	-17	-17
Net primary production	8	8
Chlorophyll	3	3
Nitrate	-6	-6
Gross secondary production	10	10
TEP	17	16
Phytoplankton filtered by filter feeders	35	34
Zooplankton filtered by filter feeders	20	19
Suspension feeders	13	12
Mass present in benthos	15	15

Table 2

	Array layout	Farm spacing horizontally (x) and vertically (y)	Farm layout	Turbine spacing
Scenario 1	4 rows x 10 farms	5 km (x and y)	20 rows x 6	800 m

			turbines	
Scenario 2	4 rows x 5 farms	10 km (x) 5 km (y)	20 rows x 6 turbines	800 m
Scenario 3	4 rows x 10 farms	10 km (x) 5 km (y)	20 rows x 6 turbines	800 m
Scenario 4	4 rows x 5 farms	10 km (x) 5 km (y)	20 rows x 12 turbines	800 m
Scenario 5	4 rows x 10 farms	5 km (x and y)	20 rows x 3 turbines	800 m

Table 3

Hs (m)	0-1	1-2	2-3	3-4	4-5	5-6	6-7	7-8	8-9	9-10	10-11	>11
>6	0	0	0	0	0	0	0	0	0	0	0	0
5.5-6	0	0	0	0	0	0	0	0	0	0	0	0
5-5.5	0	0	0	0	0	0	0	0.12	0.08	0	0	0
4.5-5	0	0	0	0	0	0	0.01	0.18	0	0	0	0
4-4.5	0	0	0	0	0	0	0.18	0.11	0	0	0	0
3.5-4	0	0	0	0	0	0.08	0.62	0.14	0.01	0	0	0
3-3.5	0	0	0	0	0	0.75	0.95	0.14	0.07	0.01	0	0
2.5-3	0	0	0	0	0.04	3.36	0.83	0.18	0.03	0	0	0
2-2.5	0	0	0	0	1.38	5.32	0.86	0.13	0	0	0	0
1.5-2	0	0	0	0.36	10.82	7.2	1.43	0.13	0	0	0	0
1-1.5	0	0	0	6.82	14.25	4.76	1.03	0.23	0.11	0	0	0
0.5-1	0	0	0.85	18.51	8.21	1.86	0.2	0.08	0	0	0	0
0-0.5	0	0	1.57	4.04	1.54	0.46	0.01	0	0	0	0	0
					Tz (s)							

Table 4

	Array layout	**Average reduction in H_s (%)**	**Maximum reduction in H_s (%)**
Scenario 1	4 rows x 10 farms, 5km spacing, 4800 turbines	5.87	9.58

Scenario 2	4 rows x 5 farms, 10 km spacing, 2400 turbines	4.30	8.62
Scenario 3	4 rows x 10 farms, 10km spacing, 4800 turbines	4.51	9.23
Scenario 4	4 rows x 5 farms, 10km spacing, 4800 turbines	5.43	9.65
Scenario 5	4 rows x 10 farms, 5km spacing, 2400 turbines	4.71	8.68

Table 5

Wind speed (ms^{-1})	**Wind direction**	**Average reduction in H_s (%)**	**Maximum reduction in H_s (%)**
5	**Southerly**	5.30	8.78
10	**Southerly**	3.46	7.10
20	**Southerly**	2.53	6.37
9 (10% reduction from 10ms^{-1})	**Southerly**	3.73	7.30
10	**Westerly**	3.57	7.32

Highlights

- We modeled the impact on waves, sound and biogeochemistry of an offshore wind-turbine array
- All three models suggested relatively weak environmental changes
- Most changes occurred within the turbine array, with small changes in tens of km outside the array
- Combining, we found different combinations of changes within the array that may affect marine life
- Further work is required, including additional mechanisms and different hydrographic settings

Figure 1

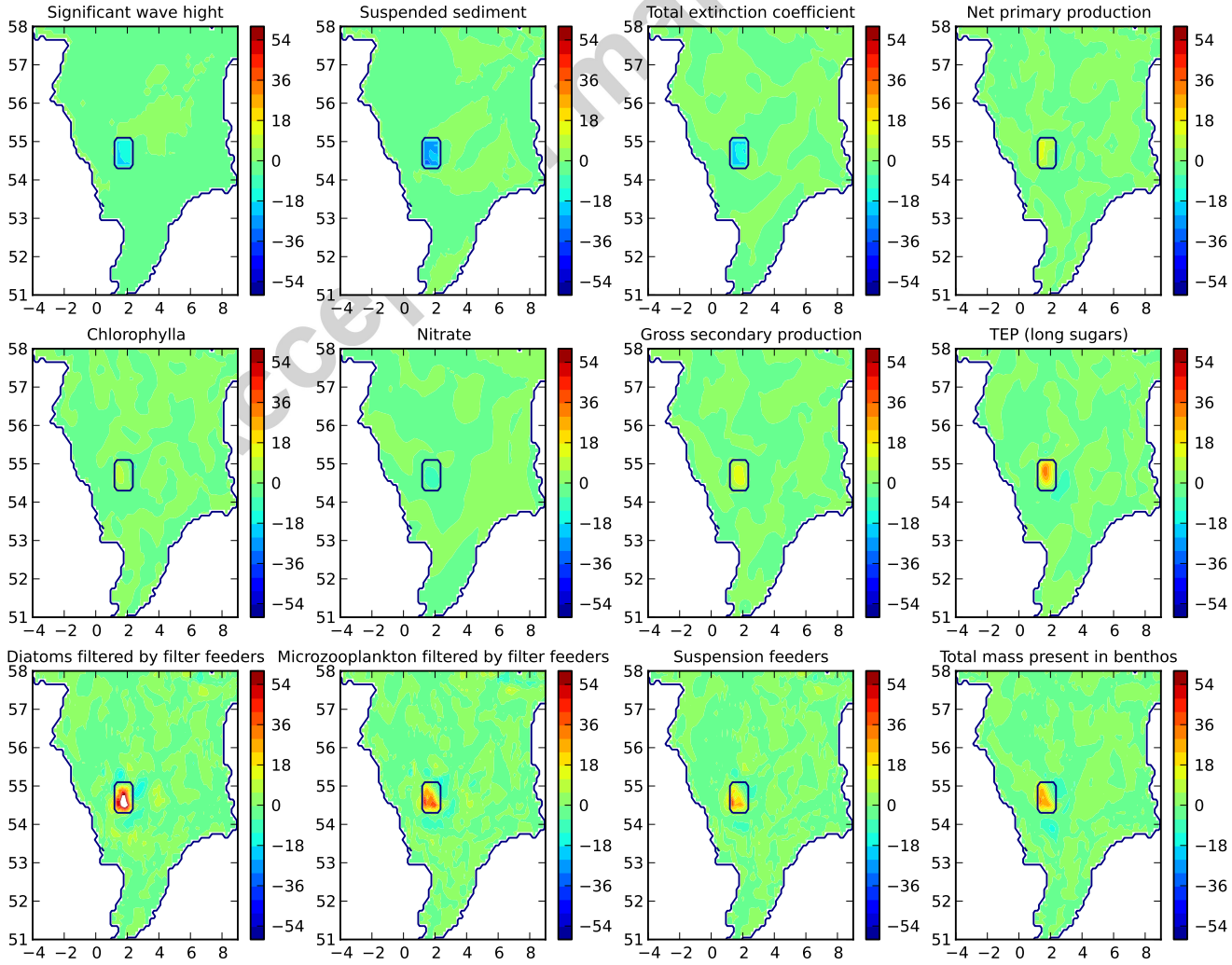

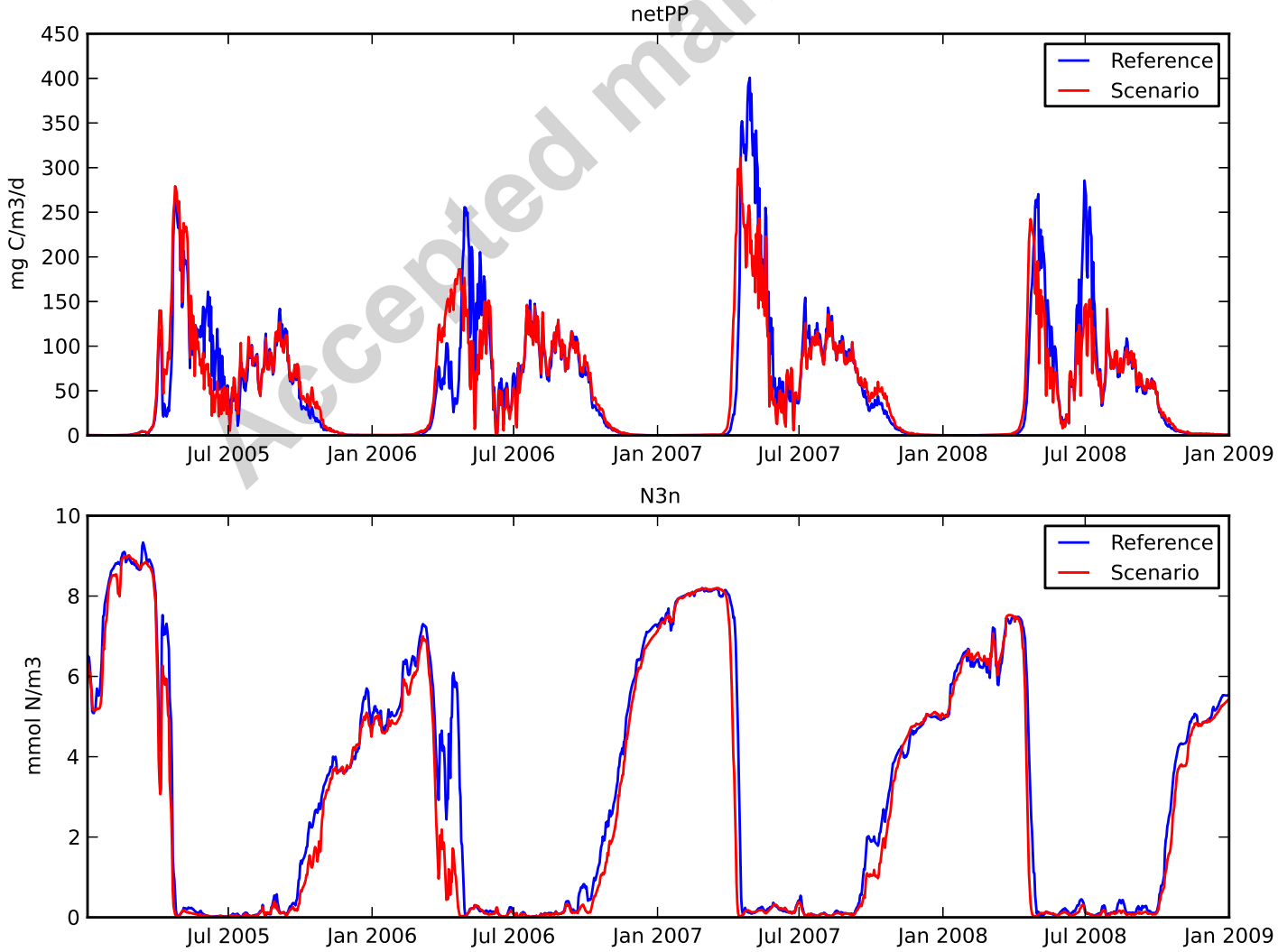

Figure 3

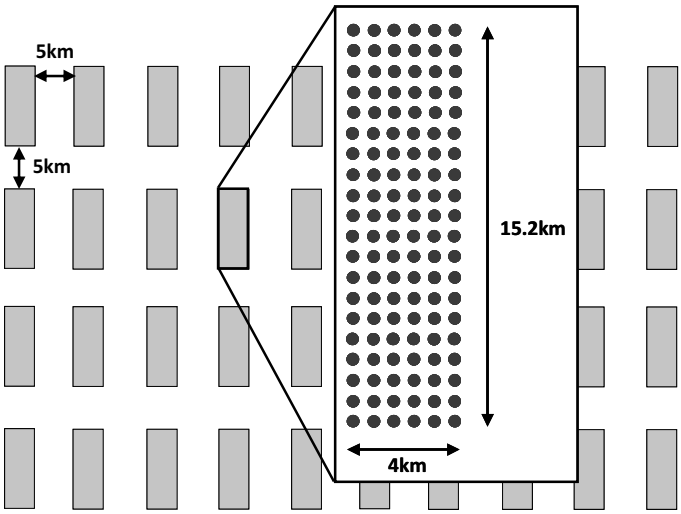

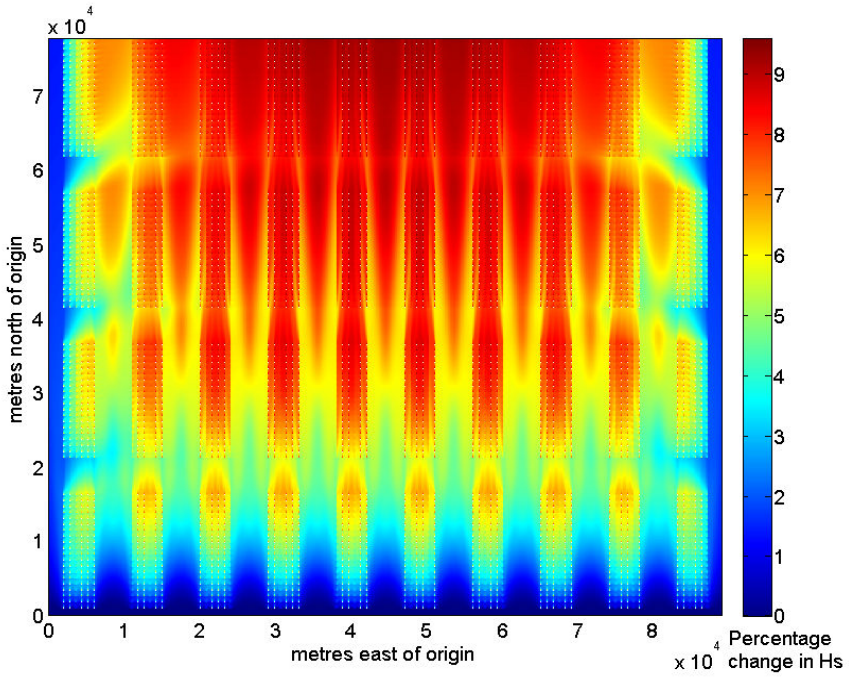

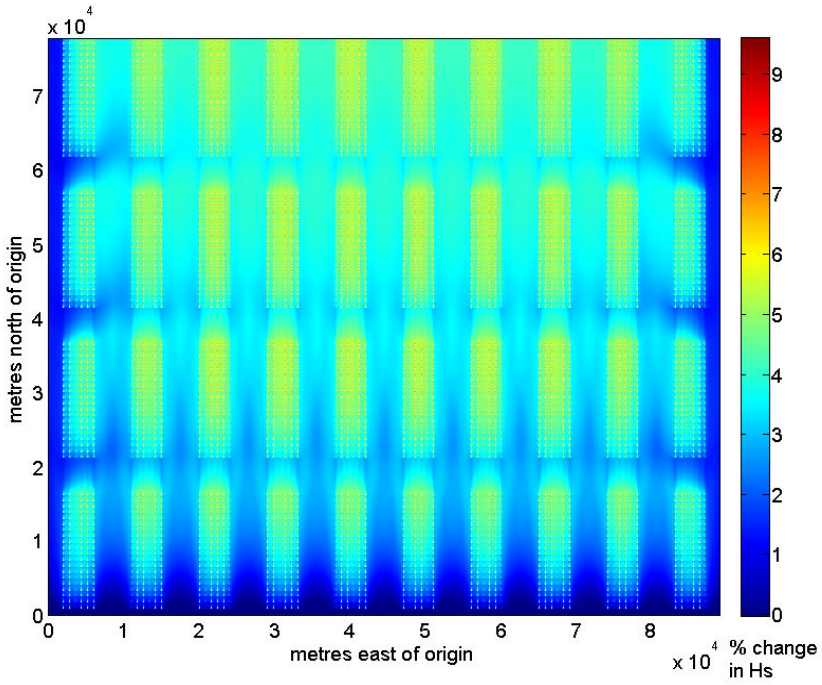

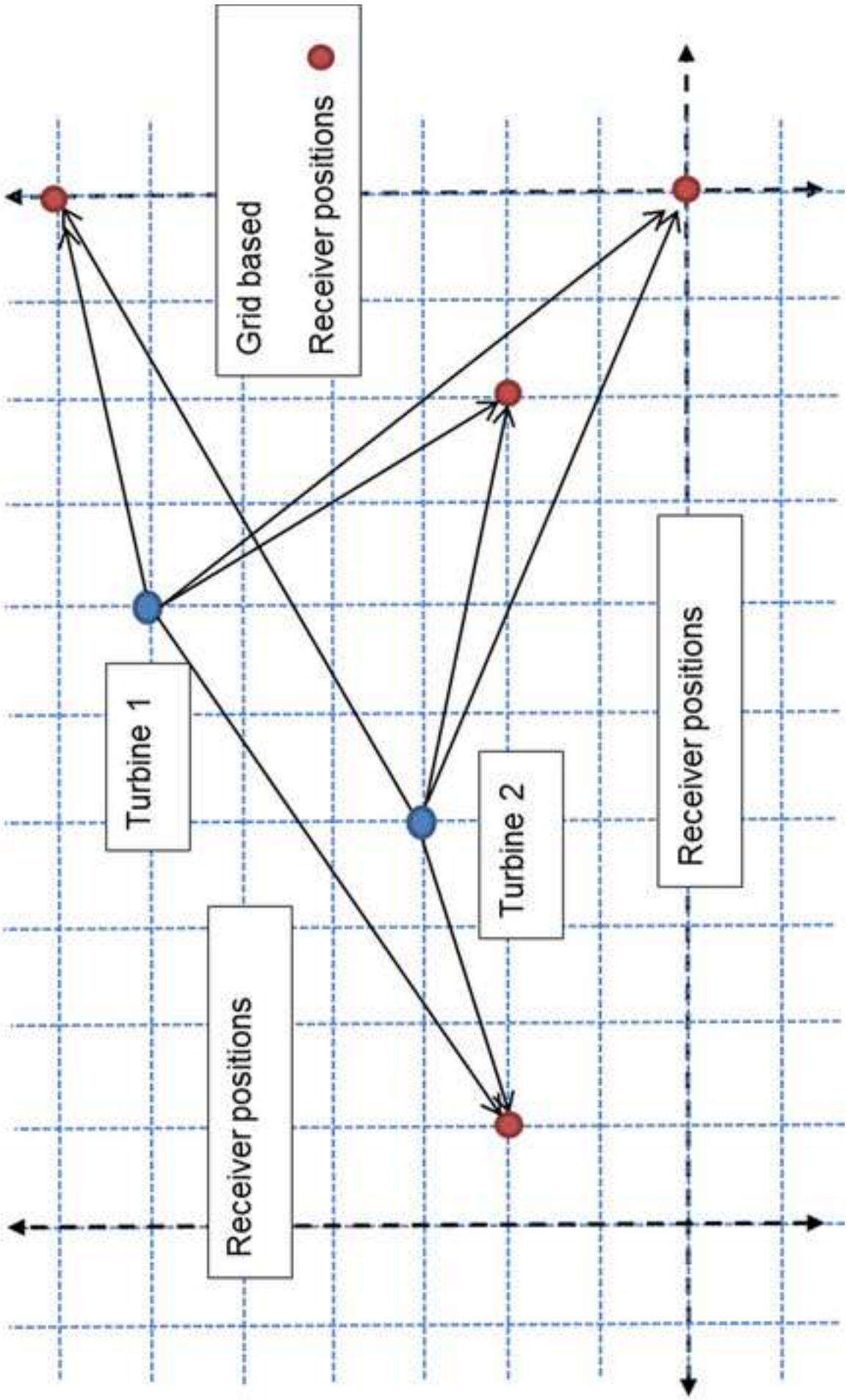
Grid based
Receiver positions
Turbine 1
Turbine 2
Receiver positions
Receiver positions

Figure 6

Figure 7

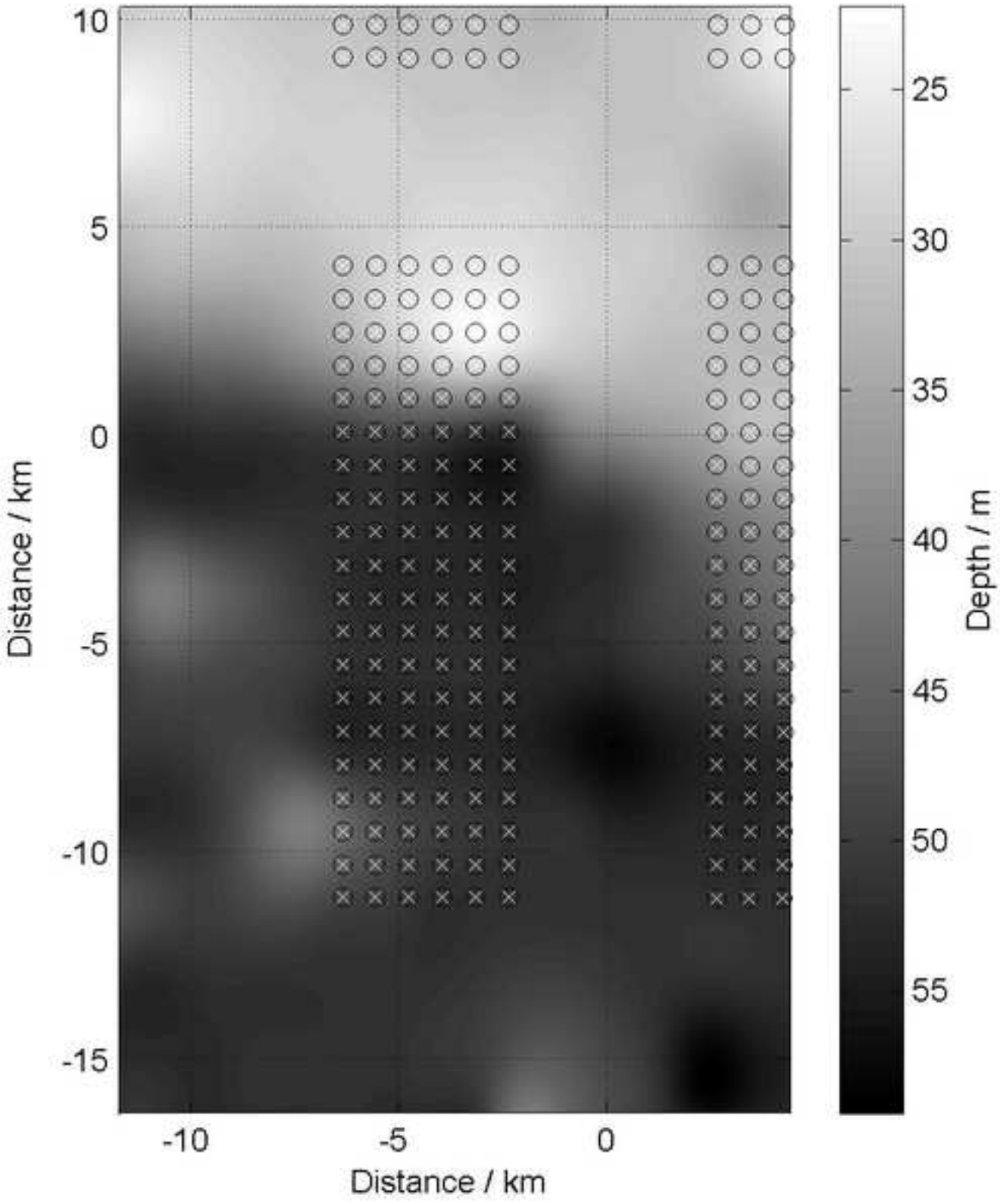

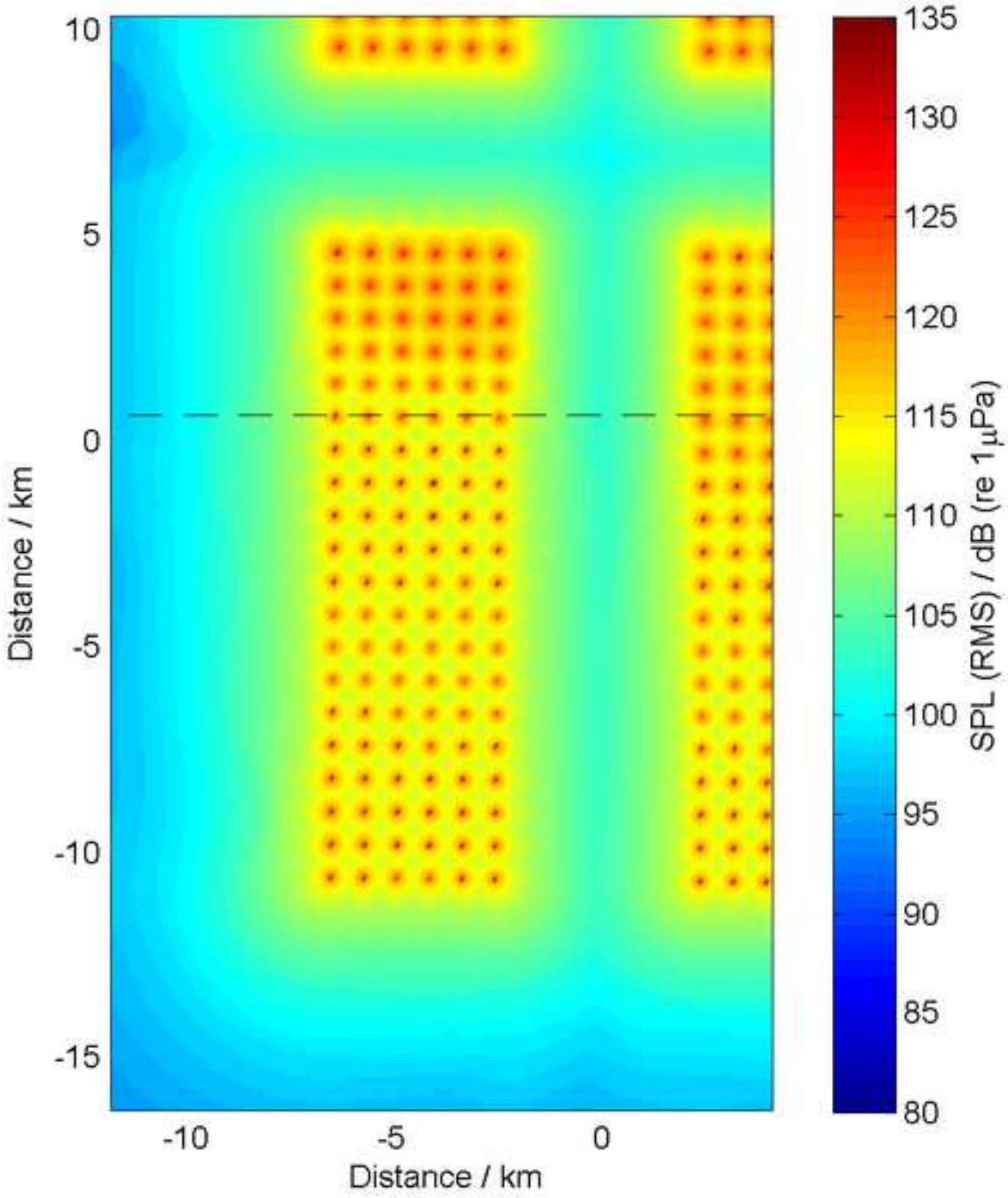

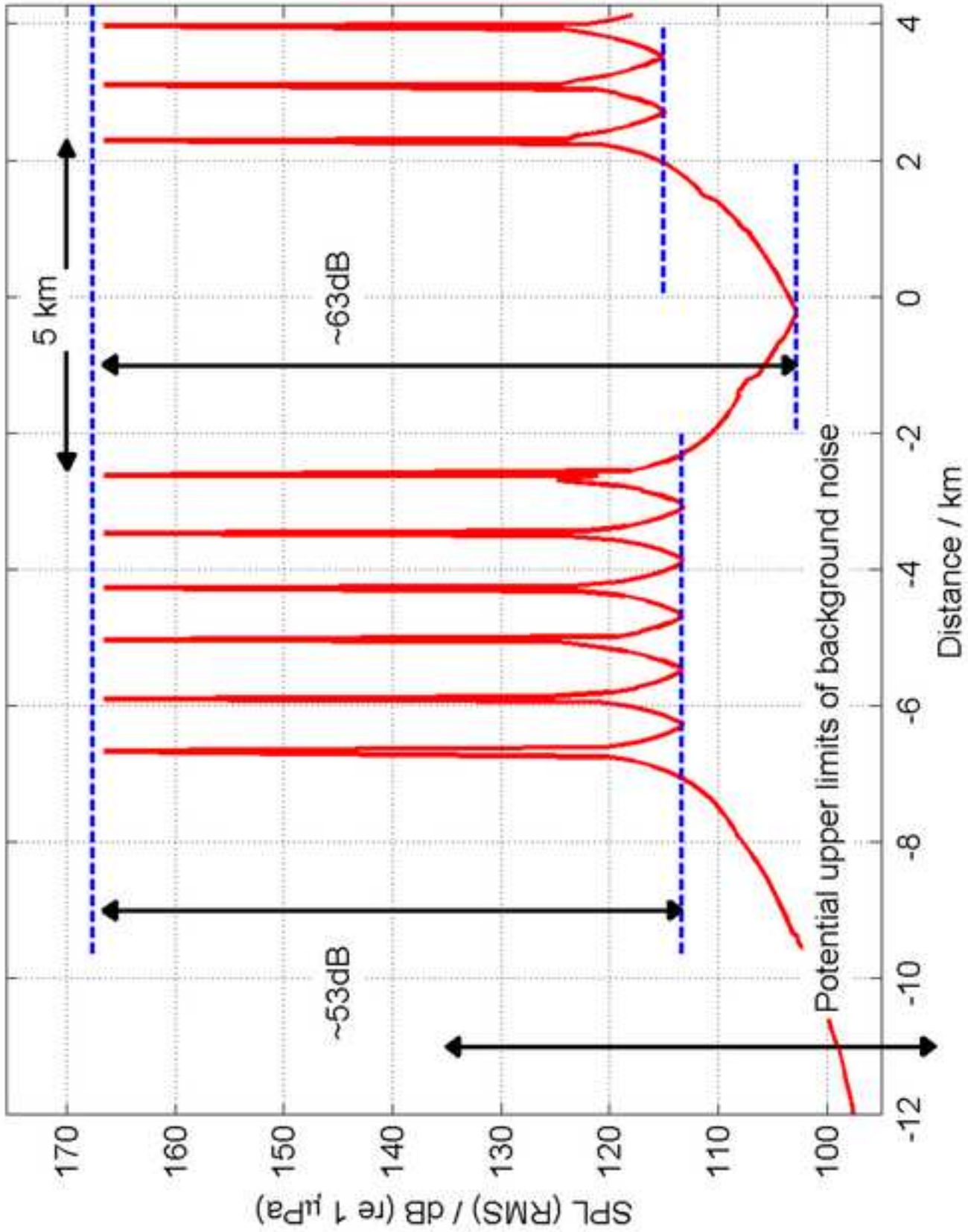
5 km
~63dB
~53dB
Potential upper limits of background noise
SPL (RMS) / dB (re 1 μPa)
Distance / km
170
160
150
140
130
120
110
100
-12
-10
-8
-6
-4
-2
0
2
4

Figure 9

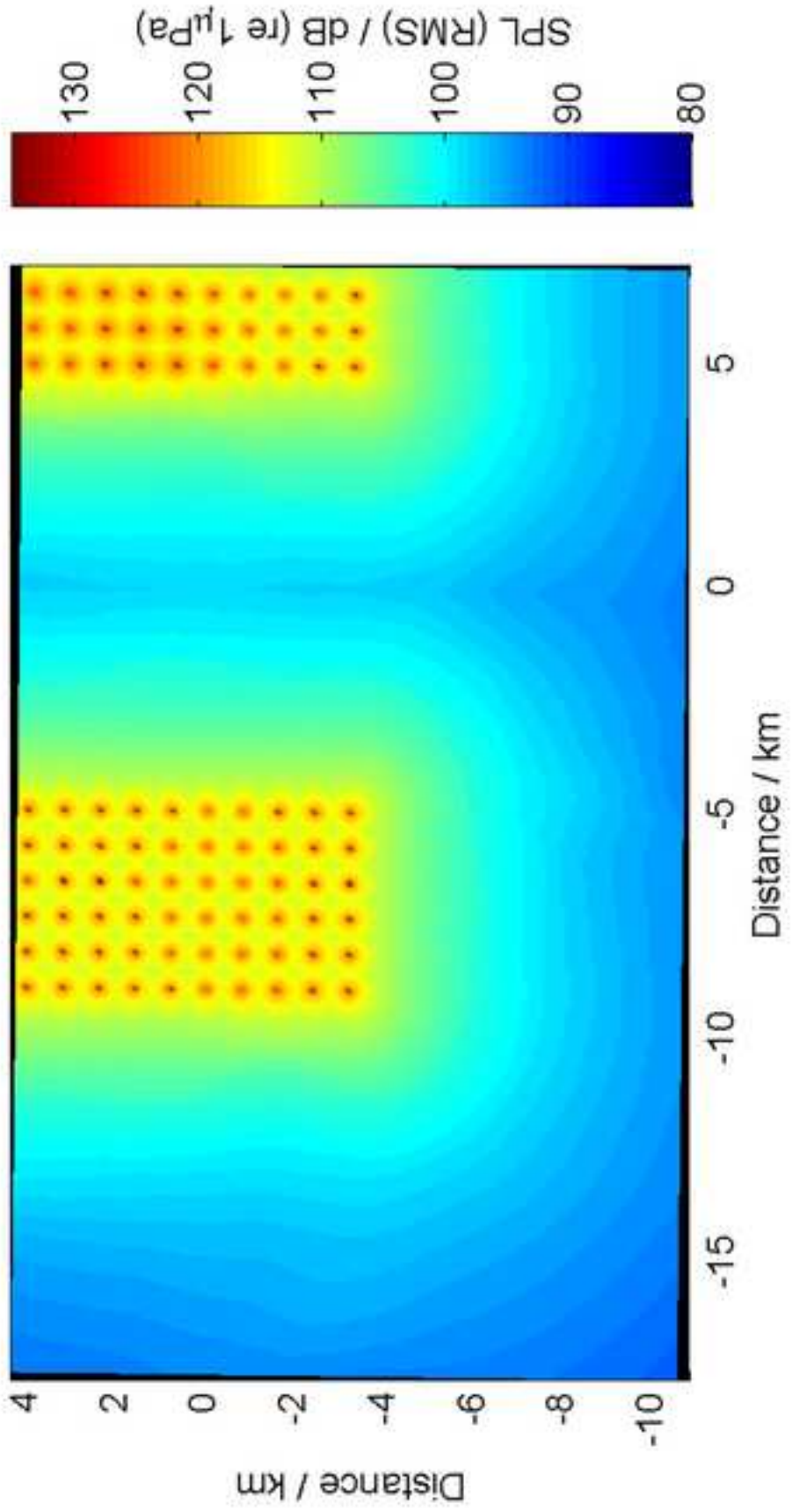
SPL (RMS) / dB (re 1μPa)
130
120
110
100
90
80
Distance / km
5
0
-5
-10
-15
Distance / km
4
2
0
-2
-4
-6
-8
-10

Figure 10

Figure 11